Chapter 29
Analysis on the Influence of Guidance Mode on the Motion Characteristics of Angular Contact Ball Bearing Cage

Xiaohong Zhang, Ke Yan, Mingkai Wang, Jun Hong, and Yongsheng Zhu

Abstract The motion characteristics of cage play a vital role in the service performance of bearing. The unstable movement of cage will lead to its wear and fracture, and the sliding of cage will also aggravate the wear and shorten the life of bearing. Moreover, the influence of the cage guidance mode on the cage motion characteristics cannot be ignored. In this regard, by means of dynamics analysis methods, the impact of the cage guidance mode on the motion characteristics of angular contact ball bearing cage is investigated by comparing the deviation ratio of vortex velocity of centroid and slip rate for cage under different working conditions. The results show that the cage stability is the best with an outer race guidance, the cage slip rate is the smallest with an inner race guidance, and the cage has poor stability and large slip rate with a ball guidance whether the bearing is subjected to unidirectional load or combined load. This research provides certain reference value for the optimization design and practical engineering application of rolling bearing cage.

Keywords Angular contact ball bearing · Cage guidance mode · Cage stability · Cage slip rate

29.1 Introduction

As a key basic component of the mechanical system, rolling bearings are used to transmit motion form and play a supporting role in rotating machinery. While, the

X. Zhang · K. Yan (✉) · M. Wang · J. Hong · Y. Zhu
Key Laboratory of Education Ministry for Modern Design and Rotor-Bearing System, Xi'an Jiaotong University, Xi'an 710049, China
e-mail: yanke@mail.xjtu.edu.cn

X. Zhang
e-mail: xh_zhang1206@stu.xjtu.edu.cn

J. Hong
e-mail: jhong@mail.xjtu.edu.cn

Y. Zhu
e-mail: yszhu@mail.xjtu.edu.cn

cage is the basic element of the rolling bearing, and its stability during operation plays a crucial role in the service performance of the bearing, which in turn affects the safety and reliability of the whole mechanical equipment. The instability of cage will lead to friction torque fluctuations, and produce serious transient forces, as well as aggravate the friction and wear of the cage, and result in whistling noise, which will make the bearing lose accuracy and even cause the spindle bearing stuck, bringing unpredictable harm [1–4]. The skiding phenomenon of rolling bearing not only aggravates friction and wear, but also raises the temperature of the lubricating oil, resulting in the thermal deformation of the bearing raceway, and the radial clearance of the bearing is significantly reduced, thus destroying the accuracy of bearing operation [5]. Therefore, the research on the performance of rolling bearing cages has always been a widespread concern of scholars at home and abroad. Deng et al. [6–9], analyzed the influence of cage pocket clearance, guide clearance and pocket shape on the friction torque and vibration of bearing, as well as the cage centroid eccentricity for angular contact ball bearings by means of dynamic analysis methods. Yao et al. [10], analyzed the effect of the cage pocket radius clearance on system dynamic error, the collision force between steel ball and cage, and the steel ball skidding by establishing a multi-body contact dynamics model about the system of ball bearing and crank slider mechanism. In recent work [11], the lubrication collision between rolling elements and cage pocket was considered, based on the dynamic model of rolling bearing, the influence of the working conditions such as bearing preload, radial load, inner ring speed and the structure parameter such as guide pocket clearance ratio on the dynamic characteristics of precision bearing cages were analyzed. Takashi et al. [12] established a simple theory about the instability of cage, proposed the critical friction coefficient of cage, and found that the increase of the friction coefficient would lead to the motion instability of the cage.

At present, although a great deal of discussion has been made on the cage characteristics, there is still a lack of research on the effects of cage structure, especially the guidance mode, on its operating characteristics. In view of this, with the help of the multi-body contact dynamics analysis software ADAMS, this paper analyzes the influence of the cage with different guidance mode on the motion characteristics of angular contact ball bearing cage under different working conditions, so as to provide certain reference for the optimal design and practical application of the bearing.

29.2 Cage Theory

29.2.1 Cage Guidance Mode

As the core part of the bearing, the cage mainly plays the role of evenly isolating the rolling elements and guiding their operation. The cage of the separation type bearing combines the rolling elements into a component to facilitate installation and prevent the strictly grouped rolling elements from being confused with each other [13].
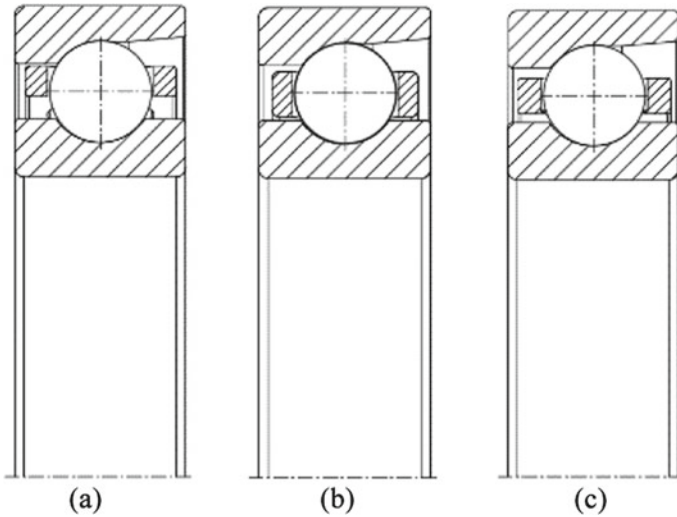
Fig. 29.1 Cage guidance mode: **a** outer race guidance; **b** inner race guidance; **c** ball guidance

When the bearing is working, the cage is driven by different components inside the bearing. In the traditional sense, the cage can be divided into three structures according to the guidance mode: outer race guided cage, inner race guided cage and ball guided cage. The specific structure is shown in Fig. 29.1. With an outer race guidance, cage operation is driven by the outer ring rib of bearing. With an inner race guidance, cage operation is driven by the inner ring rib of bearing. With a ball guidance, cage operation is driven by the gap between the cage pocket and the steel ball. The purpose of cage guidance is to make the cage 'rely on' in the circumferential and radial directions, so that the movement of cage tends to be stable without vortex.

29.2.2   Theory of Stability and Slip Characteristics of Cage

Ghaisa et al. [14], took the deviation ratio of cage centroid vortex velocity as the stability criterion of cage, which is defined the ratio of standard deviation of cage center of mass velocity vector to its mean velocity.

$$\sigma_v = \frac{\sqrt{\sum_{i=1}^{i=n} (v_i - v_m)^2 /(n-1)}}{v_m} \tag{29.1}$$

where v_i is the velocity of the center of mass of cage at moment i/m s^{-1}, v_m is the average velocity of the center of mass of cage/m s^{-1}, n is the number of samples. The

Fig. 29.2 Kinematics
relationship of angular
contact ball bearing
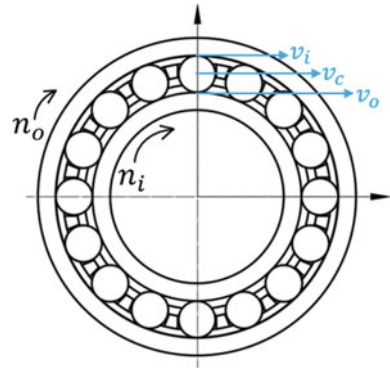
smaller the value of σ_v, which shows that the change of cage whirl speed is smaller
and then the stability of cage motion is better. Otherwise, the result is worse.

At the same time, the cage rotation speed can be measured to judge whether the
bearing is slipping or not. And the cage slip rate is defined as the error between the
actual rotation speed and the theoretical rotation speed of cage. The theoretical speed
of cage can be calculated from the kinematics relationship of angular contact ball
bearing, and the actual speed can be directly extracted from the dynamic simulation
results (Fig. 29.2).

When the inner ring and outer of bearing rotate at the same time, and they have
the same contact angle α, the linear velocity v_i and v_o of the contact points between
steel ball and raceway of inner ring and outer are:

$$v_i = \frac{\pi}{60} n_i d_m \left(1 - \frac{D \cos \alpha}{d_m} \right) \tag{29.2}$$

$$v_o = \frac{\pi}{60} n_o d_m \left(1 + \frac{D \cos \alpha}{d_m} \right) \tag{29.3}$$

where n_i is inner ring rotation speed/r min^{-1}, n_o is outer ring rotation speed/r min^{-1},
d_m is diameter of the bearing pitch circle, and D is diameter of the steel ball.

If there is no serious sliding at the contact point in the ring raceway, the linear
velocity of cage and steel ball is the average linear velocity of the contact point
between the ring raceway and the steel ball of bearing, and the linear velocity of cage
is

$$v_c = \frac{\pi}{120} n_i d_m \left(1 - \frac{D \cos \alpha}{d_m} \right) + \frac{\pi}{120} n_o d_m \left(1 + \frac{D \cos \alpha}{d_m} \right) \tag{29.4}$$

due to

$$v_c = \frac{1}{2} w_c d_m = \frac{\pi n_c d_m}{60} \tag{29.5}$$

the theoretical cage speed

$$n_c = \frac{n_i}{2}\left(1 - \frac{D\cos\alpha}{d_m}\right) + \frac{n_o}{2}\left(1 + \frac{D\cos\alpha}{d_m}\right) \tag{29.6}$$

substitute $\gamma = \frac{D\cos\alpha}{d_m}$ into Eq. (29.6), we can get

$$n_c = \frac{1}{2}\left[n_i(1 - \gamma) + n_o(1 + \gamma)\right] \tag{29.7}$$

the cage slip rate is

$$S_c = \frac{n_c - n_m}{n_c} \times 100\% \tag{29.8}$$

where n is the actual rotation speed of cage/r min^{-1}. The high slip rate indicates that the actual rotation speed of cage differs greatly from the theoretical, which is easy to cause the wear between cage and guidance ring, as well as the heat between steel ball, guidance ring and cage, even result in bearing failure [15].

29.3 Dynamics System Model of Bearing

29.3.1 3-D Assembly Model of Bearing

In this paper, the angular contact ball bearing model is 7014C/P5, which is taken as the research object. The basic structure parameters of the bearing are shown in Table 29.1, and the material parameters are shown in Table 29.2. After the bearing parts are completed in the modeling software, they are assembled. The three-dimensional assembly models for bearings with different guidance mode cage are shown in Fig. 29.3, then they are exported after interference checking.

29.3.2 Boundary Conditions

The bearing model is imported into the multi-body contact dynamics analysis software, and the kinematic pairs between the bearing components are set according to the kinematic relationships of rolling bearing. The outer ring and the ground are set

Table 29.1 Basic structure parameters of the bearing

Structure parameters	Value
Bearing outer diameter (D/mm)	110
Bearing inner diameter (d/mm)	70
Bearing width (B/mm)	20
Bearing pitch diameter (D_p/mm)	89.944
Radius of curvature of the race groove (r_i/r_o/mm)	6.2
Rolling element diameter (D_b/mm)	11.906
Rolling element number (Z)	20
Cage pocket diameter (D_{cp}/mm)	12.5
Limit speed (n_i/r min^{-1})	8000

Table 29.2 Material parameters of the bearing

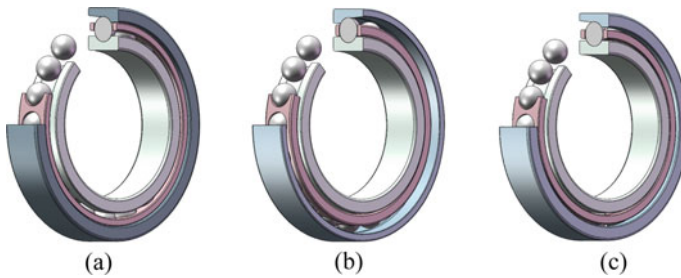|	Elastic modulus E/Mpa	Poisson's ratio v	Density ρ/kg mm^{-3}
Rolling elements and two rings	2.08×10^5	0.3	7.83×10^{-6}
Cage	3.55×10^3	0.1	1.32×10^{-6}

Fig. 29.3 3-D assembly models of angular contact ball bearing: **a** assembly model with an outer race guided cage; **b** assembly model with an inner race guided cage; **c** assembly model with a ball guided cage

fixed pairs, the cage and the outer ring are set plane pairs, and the inner ring is driven by a single degree of freedom. The contact parameters between bearing parts are set as shown in Table 29.3, and the dynamic simulation model established is shown in Fig. 29.4.

Due to the complexity of the established model, the following assumptions should be made:

Table 29.3 Contact parameters between bearing parts

	Outer ring and rolling element	Inner ring and rolling element	Cage and rolling element
Contact stiffness	2.9154×10^5	2.7071×10^5	2.5477×10^5
Force exponent	1.5	1.5	1.5
Damping	50	50	50
Penetration depth	0.01	0.01	0.01
Static coefficient	0.2	0.2	0.2
Dynamic coefficient	0.1	0.1	0.1
Stiction transition vel.	10	10	10
Friction transition vel.	20	20	20

Fig. 29.4 Dynamic simulation model of angular contact ball bearing
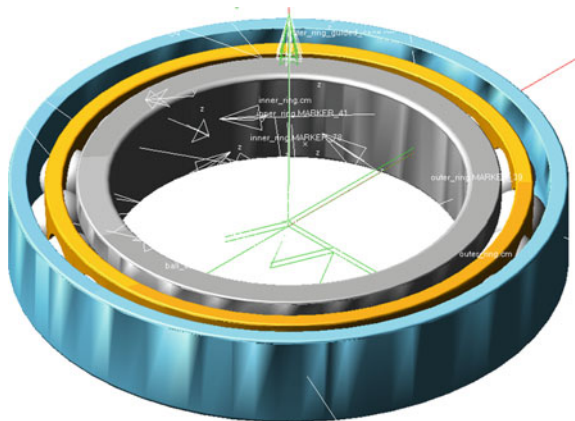
(1) It is assumed that each part of the bearing is a rigid body, the flexible deformation generated in the process of motion is ignored. And if there is contact between bearing components, elastic deformation occurs.

(2) The center of form coincides with the center of mass of the bearing components.

(3) The internal temperature of bearing adopts the software default value.

29.4   Cage Motion Characteristics Analysis

29.4.1   Cage Stability Analysis

When the outer ring of the bearing is fixed, as well as the unidirectional load and combined load are applied to the inner ring respectively, the deviation ratio of cage centroid vortex velocity with three guidance mode is obtained.

Figure 29.5 shows the deviation ratio of cage centroid vortex velocity with three guidance mode. Pure axial load is applied to the inner ring, and the bearing speed is 1000 r/min. It can be found that the deviation ratio of cage centroid vortex velocity raises with the increase of axial load. Among them, the deviation ratio of cage centroid vortex velocity with an outer race guidance is the smallest and the fluctuation range is small, the deviation ratio with a ball guidance cage is 0.006 larger than that of the outer race and the fluctuation range is larger. The deviation ratio with an inner race guidance cage shows a sharp fluctuation, and the average value is between that of the outer race and the ball, the deviation ratio raises significantly with the increase of axial load. Ultimately, the deviation ratio with an inner race guidance cage raises 0.02 in the range of the axial load change.

Figure 29.6 shows the deviation ratio of cage centroid vortex velocity with three guidance mode. Pure radial load is applied to the inner ring, and the bearing speed is 1000 r/min. It can be found that the deviation ratio of cage centroid vortex velocity with three guidance mode raises with the increase of the radial load, and the fluctuation range is about 0.005., the deviation ratio with an inner race guidance cage is 0.003 larger than that of the outer race, and the deviation ratio with a ball guidance cage is 0.002 larger than that of the inner race.

Figure 29.7 shows the deviation ratio of cage centroid vortex velocity with three guidance mode, applying an axial load of 100 N and a radial load of 10,000 N to the inner ring. It is observed that the deviation ratio of cage centroid vortex velocity

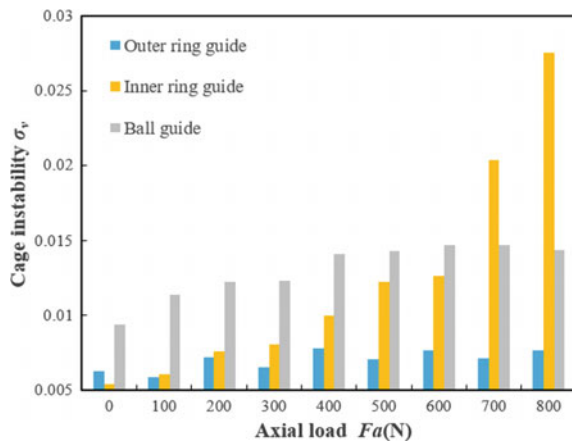**Fig. 29.5** Cage instability versus axial load for different guidance mode

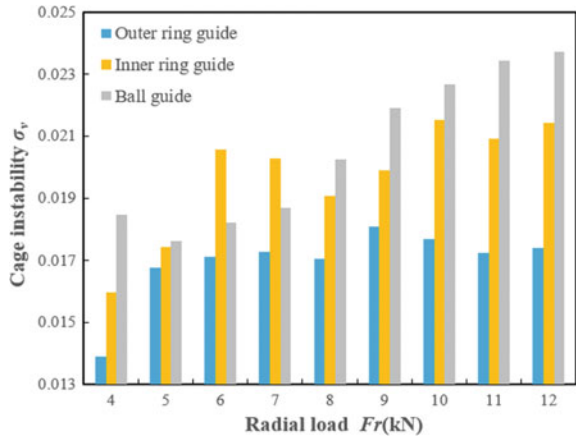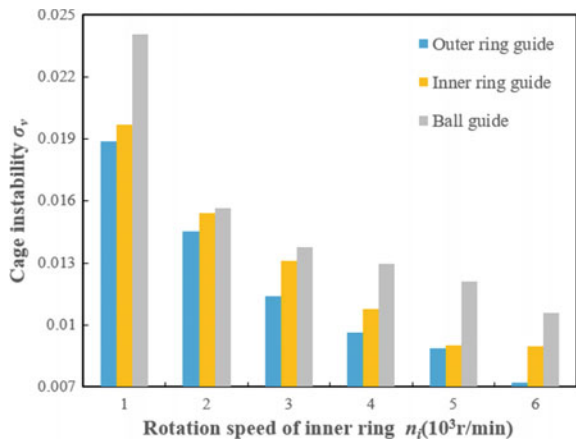**Fig. 29.6** Cage instability versus radial load for different guidance mode

Fig. 29.7 Cage instability versus rotational speed of inner ring for different guidance mode

with three guidance mode reduces with the increase of the rotation speed of inner ring, and the fluctuation range is around 0.1. Among them, the deviation ratio of cage centroid vortex velocity with an outer race guidance is the smallest, the deviation ratio with an inner race guidance cage is 0.001 larger than that of the outer race, and the deviation ratio with a ball guidance cage is 0.002 larger than that of the inner race.

The results show that, the stability of the outer race guided cage is the best and that of the ball guided cage is the worst with changing the external working conditions when the angular contact ball bearing is under unidirectional load or combined load conditions. While, the deviation ratio of cage centroid vortex velocity with an inner race guidance fluctuates sharply with the change of the load when the bearing is applied unidirectional load. Just because the cage with different guidance mode have different installation position, and the contact force on cage varies greatly during bearing operation. The outer race guided cage is close to the outer ring, which is

relatively less affected by the rotation of inner ring and the movement of steel balls. The ball guided cage is subject to more discontinuous contact and collision with steel balls. The inner race guided cage is closer to the inner ring, which is greatly affected by the rotation of inner ring.

29.4.2 Cage Slip Analysis

When the outer ring of the bearing is fixed, as well as the unidirectional load and combined load are applied to the inner ring respectively, the slip rate of cage with three guidance mode is obtained.

Figure 29.8 shows the slip rate of cage with three guidance mode. Pure axial load is applied to the inner ring, and the bearing speed is 1000 r/min. It can be found that the cage slip rate reduces with the increase of axial load. Among them, the cage slip rate with a ball guidance is the highest, followed by the outer race guided cage, and the cage slip rate with an inner race guidance is the lowest. In addition, the slip rate of outer race guided cage fluctuates greatly, while the slip rate change trend of inner race guided cage and ball guided cage is relatively stable.

Figure 29.9 shows the slip rate of cage with three guidance mode. Pure radial load is applied to the inner ring, and the bearing speed is 1000 r/min. It can be found that the cage slip rate raises with the increase of radial load. Among them, the cage slip rate with a ball guidance is the highest and the value increase 0.7% in the range of the radial load change. The cage slip rate with an outer race guidance is lower, the value is 0.5% smaller than that of the ball guidance. The cage slip rate with an inner race guidance is the lowest, the value is 0.1% smaller than that of the outer race guidance, while the fluctuation range is wider and the value is up to 0.5%. The results show that, the stability of cage is the best with the outer race guidance, the slip rate of cage is the lowest with the inner race guidance, the stability is bad and

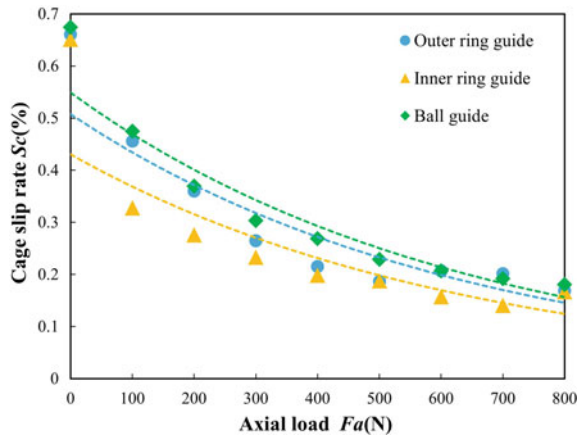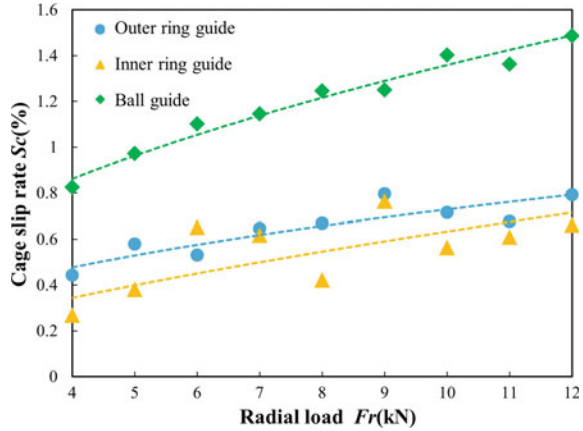**Fig. 29.8** Cage slip rate versus axial load for different guidance mode

**Fig. 29.9** Cage slip rate versus radial load for different guidance mode

the slip rate is high of cage with the ball guidance, when the angular contact ball bearing is applied pure radial load.

Figure 29.10 shows the slip rate of cage with three guidance mode, applying an axial load of 100 N and a radial load of 10,000 N to the inner ring. It can be found that the cage slip rate shows great difference with changing inner ring speed. The cage slip rate reduces with the outer race guidance and the ball guidance under the increase of inner ring rotation speed. Moreover, there is a decrease at low rotation speed and an increase at high rotation speed of cage slip rate with an inner race guidance. Among them, the cage slip rate is the lowest with an inner race guidance. The cage slip rate with an outer race guidance is higher, the average value is 0.1% larger than that of the inner race guidance. The cage slip rate with a ball guidance is the highest, the average value is 0.6% larger than that of the outer race guidance.

The results show that, the slip rate of the inner race guided cage is the lowest and the slip rate of the ball guided cage is the highest with changing the external working

Fig. 29.10 Cage slip rate versus rotational speed of inner ring for different guidance mode
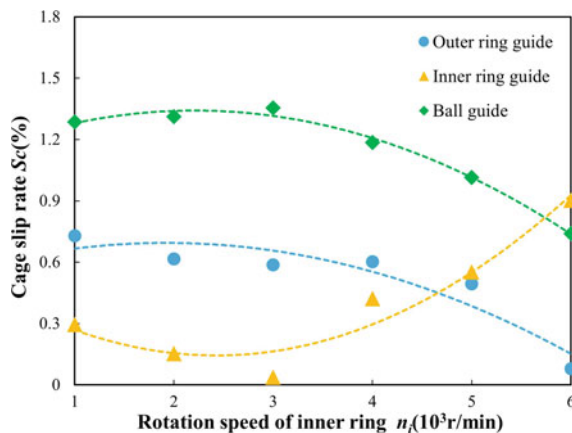
conditions when the angular contact ball bearing is under unidirectional load or combined load conditions. Just because the movement range of three guidance mode cage is different during the bearing motion. The inner race guided cage is close to the inner ring, affected by the rotation of inner ring, the contact between cage and guide ring is relatively short. While the ball guided cage is subject to multiple discontinuous contact and collision with steel balls.

29.5 Conclusions

By the 3-D multi-body contact dynamics simulation of the angular contact ball bearing with three guidance mode cages, the deviation ratio of cage centroid vortex velocity and slip rate of cage are analyzed under different working conditions. The following conclusions can be drawn based on the model analysis:

(1) When the angular contact ball bearing is subjected to unidirectional load, the stability of cage deteriorates gradually as the load increases. Among them, the cage stability is the best with an outer race guidance, followed by an inner race guidance, and the cage stability is the worst with a ball guidance.

(2) When the angular contact ball bearing is subjected to combined load, the stability of cage improves gradually with the increase of the rotation speed of inner ring. Among them, the cage stability is still the best with an outer race guidance, followed by an inner race guidance, and the cage stability is the worst with a ball guidance.

(3) Whether the angular contact ball bearing is subjected to unidirectional load or combined load, the cage slip rate is the highest with a ball guidance, followed by the outer race guidance, and the cage slip rate is the lowest with an inner race guidance.

References

1. Sathyan, K., Hsu, H.Y., Lee, S.H., et al.: Long-term lubrication of momentum wheels used in spacecrafts-an overview. Tribol. Int. **43**(1–2), 259–267 (2010)
2. Sathyan, K., Gopinath, K., Lee, S.H., et al.: Bearing retainer designs and retainer instability failures in space-craft moving mechanical systems. Tribol. Trans. **55**(4), 503–511 (2012)
3. Zhang, T., Chen, X., Gu, J., Li, Q., et al.: Research progress on cage stability of high speed angular contact ball bearings. Acta Aeronautica et Astronautica Sinica **39**(7), 32–44 (2018). [in Chinese]
4. Li, Q.Q., Chen, X.Y., Zhang, T., et al.: Experimental research on cage dynamic characteristics of angular contact ball bearing. Mech. Ind. **20**(2) (2019)

5. Jin, Q.C., Zhang, Q., Luo, J., et al.: Research progress on skidding experimental analysis of rolling bearings. Mach. Tool Hydraul. **47**(22), 165–168 (2019)
6. Deng, S.E., Li, X.L., Wang, J.G., et al.: Frictional torque characteristic of angular contact ball bearings. J. Mech. Eng. **47**(5), 114–120 (2011). (in Chinese)
7. Deng, S.E., Hua, X.W., Zhang, W.H.: Analysis on friction torque fluctuation of angular contact ball bearing in gyro motor. J. Aerosp. Power **33**(7), 1713–1724 (2018). (in Chinese)
8. Deng, S.E., Lu, Y.J., Hua, X.W., et al.: Vibration characteristics of four-column angular contact ball bearings. J. Vib. Shock **36**(9), 1–6 (2017). (in Chinese)
9. Deng, S.E., Hao, J.J., Teng, H.F., et al.: Dynamics analysis on cage of angular contact ball bearings. Bearing **10**, 1–5 (2007). (in Chinese)
10. Yao, T.Q., Wang, L.H., Liu, X.B., et al.: Dynamics analysis on ball bearing-mechanism with clearance and impact of cage. J. Aerosp. Power **31**(7), 1725–1735 (2016). (in Chinese)
11. Yuan, Q.Q., Zhu, Y.S., Zhang, J.H., et al.: Cage dynamic characteristic of precision rolling ball bearings considering lubrication collision. J. Xi'an Jiaotong Univ. **55**(1), 110–117 (2021). (in Chinese)
12. Takashi, N., Kazuaki, M., Noriko.: A dynamic analysis of cage instability in ball bearings. J. Tribol. **140**(1) (2018)
13. Deng, S.R., Jia, Q.Y., Xue, J.X.: Design Principles of Rolling Bearings, 2nd edn. Standards Press of China, Beijing (2008). (in Chinese)
14. Ghaisas, N., Wassgren, C.R., Sadeghi, F.: Cage instabilities in cylindrical roller bearings. J. Tribol. **126**(4), 681–689 (2004)
15. Wang, L.Q.: Design and Numerical Analysis of Rolling Element Bearing for Extreme Application, 1st edn. Harbin Institute of Technology Press, Harbin (2013). (in Chinese)

Xiaohong Zhang born in 1993, is currently a Ph.D. candidate at Key Laboratory of Education Ministry for Modern Design and Rotor-Bearing System, Xi'an Jiaotong University, China. Her research interests include dynamic analysis of rolling bearings.

Ke Yan born in 1984, is currently a professor and Ph.D. candidate supervisor at Key Laboratory of Education Ministry for Modern Design and Rotor-Bearing System, Xi'an Jiaotong University, China. He received his Ph.D. degree from Shandong University, China, in 2012. His research interests include intelligent detectionsmart materialsoftware development and CFD analysis.

Mingkai Wang born in 1995, is currently a Ph.D. candidate at Key Laboratory of Education Ministry for Modern Design and Rotor-Bearing System, Xi'an Jiaotong University, China.

Jun Hong born in 1968, is currently a professor and Ph.D. candidate supervisor at Key Laboratory of Education Ministry for Modern Design and Rotor-Bearing System, Xi'an Jiaotong University, China. His main research interests include digital designhuman–machine interface design, digital assembly technology and service status online monitoring technology.

Yongsheng Zhu born in 1973, is currently a professor and Ph.D. candidate supervisor at Key Laboratory of Education Ministry for Modern Design and Rotor-Bearing System, Xi'an Jiaotong University, China. His research interests include modeling and testing technology of bearing service state and operation status monitoring, evaluation and prediction technology research.